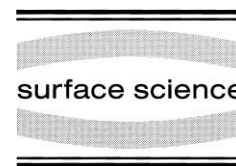




ELSEVIER

Surface Science 408 (1998) 146–159



STM observations of Ag adsorption on the Si(111)- $\sqrt{3} \times \sqrt{3}$ -Ag surface at low temperatures

Xiao Tong^a, Yasuhito Sugiura^b, Tadaaki Nagao^{a,b}, Tomohide Takami^b,
Sakura Takeda^b, Shozo Ino^b, Shuji Hasegawa^{a,b,*}

^a Core Research for Evolutional Science and Technology (CREST), The Japan Science and Technology Corporation (JST),
Kawaguchi Center Bldg., Hon-cho 4-1-8, Kawaguchi, Saitama 332, Japan

^b Department of Physics, School of Science, University of Tokyo, 7-3-1 Hongo, Bunkyo-ku, Tokyo 113, Japan

Received 4 August 1997; accepted for publication 17 February 1998

Abstract

We have systematically studied the structural evolutions during adsorption of additional Ag atoms on the Si(111)- $\sqrt{3} \times \sqrt{3}$ -Ag surface at 70 K by scanning tunneling microscopy. In the coverages less than 0.02 ML (monolayer), the Ag adatoms distribute randomly as monomers on the $\sqrt{3} \times \sqrt{3}$ -Ag surface. With coverage increase up to 0.1 ML, two-dimensional (2D) nuclei consisting of four Ag adatoms appear, the density of which is much higher at surface steps than on terraces. With being deposited further, the $\sqrt{21} \times \sqrt{21}$ -Ag domains appear by coalescing the 2D nuclei with each other. In the coverages from 0.14 to 0.20 ML, a well-ordered $\sqrt{21} \times \sqrt{21}$ -Ag superstructure is formed with $\pm 10.89^\circ$ orientations with respect to $[11\bar{2}]$ directions. The out-of-phase domain boundaries of the $\sqrt{21} \times \sqrt{21}$ phase are usually straight and along the direction of $[11\bar{2}] \pm 10.89^\circ$. An atomic structural model for the $\sqrt{21} \times \sqrt{21}$ phase has been proposed in which its unit cell contains four Ag adatoms adsorbed on the Ag trimers of the unaltered $\sqrt{3} \times \sqrt{3}$ -Ag framework. This model seems to be consistent with the 2D nuclei created at the initial stage of adsorption and also with the domain boundary structure. This model also seems to be applicable to the Au-induced $\sqrt{21} \times \sqrt{21}$ phase on the $\sqrt{3} \times \sqrt{3}$ -Ag surface. © 1998 Elsevier Science B.V. All rights reserved.

Keywords: Adsorption; Coalesce; Nucleus; Scanning tunneling microscopy; Silicon; Silver; Surface structure

1. Introduction

We have systematically studied noble-metal adsorptions on the Si(111)- $\sqrt{3} \times \sqrt{3}$ -Ag surface in a series of papers [1–13]. It is found out in these works that the systems exhibit interesting phenomena in structural [1] and electronic [5,13] changes, and also in surface electronic transport

properties [2–4,6–12]. Close correlations among them are clarified. The reason why we have chosen the $\sqrt{3} \times \sqrt{3}$ -Ag surface as a substrate is that this surface is already well solved in atomic [14,15] and electronic [16–22] structures, so that, based on such rich knowledge, we can discuss their modifications induced by additional noble-metal adsorptions. The $\sqrt{3} \times \sqrt{3}$ -Ag surface is, indeed, sensitively modified by small amounts of the adsorptions, which should be contrasted to the Si(111)- 7×7 clean surface.

* Corresponding author.

E-mail: shuji@surface.phys.s.u-tokyo.ac.jp

When a very small amount of Ag (less than approximately 0.03 monolayer, ML) adsorb on the $\sqrt{3} \times \sqrt{3}$ -Ag surface at room temperature (RT), it has been found through electrical conductance measurements that they make a metastable (supersaturated) “two-dimensional (2D) adatom gas” phase in which the Ag adatoms migrate individually with a high mobility on the surface, without nucleation [4,5]. When the amount of Ag adatoms exceeds a critical coverage, corresponding to the critical supersaturation, they begin to nucleate into three-dimensional (3D) Ag microcrystals. An almost “bare” $\sqrt{3} \times \sqrt{3}$ -Ag surface is then recovered. At the substrate temperatures below about 250 K, the surface migration and nucleation of the Ag adatoms are suppressed, so that the gas phase is condensed into a 2D solid in which the Ag adatoms periodically arrange to form a $\sqrt{21} \times \sqrt{21}$ superstructure [1,3]. We have learned from these phenomena that the activation barrier for surface migration of the Ag adatoms on the $\sqrt{3} \times \sqrt{3}$ -Ag surface is so small that the migration is not frozen out completely even at 100 K [6,3,11,12]. The adatoms seem to migrate without destroying the “smooth” $\sqrt{3} \times \sqrt{3}$ -Ag framework of the substrate surface. This is reasonable if one considers that the $\sqrt{3} \times \sqrt{3}$ -Ag surface has no dangling bonds to attain a very low surface energy [16–22]. Then it is also plausible, as clarified in the present paper, that the $\sqrt{21} \times \sqrt{21}$ superstructure induced at low temperatures is formed without breaking the $\sqrt{3} \times \sqrt{3}$ -Ag framework [3].

The $\sqrt{21} \times \sqrt{21}$ superstructure is known to be induced also by Au [2,23–25] or Cu [26] adsorption, as well as Ag, onto the $\sqrt{3} \times \sqrt{3}$ -Ag surface, though in those cases the substrate is not needed to be cooled down to lower temperatures. Their STM (scanning tunneling microscopy) images look very similar to that of the $\sqrt{21} \times \sqrt{21}$ structure induced by Ag adsorption at lower temperatures, as shown in this paper. Further, we have recently found that alkali-metal adsorptions also give rise to the $\sqrt{21} \times \sqrt{21}$ superstructure on the $\sqrt{3} \times \sqrt{3}$ -Ag surface [27]. These findings lead to an expectation that a common physical mechanism works in formation of the $\sqrt{21} \times \sqrt{21}$ superstructure.

Since there are no dangling bonds on the $\sqrt{3} \times \sqrt{3}$ -Ag surface, it is interesting to know how to make the bonds between the adatoms and the substrate. Our photoemission spectroscopy studies for the $\sqrt{21} \times \sqrt{21}$ surface induced by Au adsorption at RT have clarified that a charge transfer occurs from the adatoms into an anti-bonding surface state of the substrate [13]. This leads to a picture that the ionized adatoms make bonds with the substrate via electrons in the surface-state band that has a character of an extended state [13]. This may makes the adatoms easy to migrate along the surface.

Based on these previous studies, in-situ STM observations in the present paper have clarified the structural evolutions from the initial $\sqrt{3} \times \sqrt{3}$ -Ag surface into the $\sqrt{21} \times \sqrt{21}$ superstructure by additional Ag adsorption at low temperatures. We propose a model for the atomic arrangement of the $\sqrt{21} \times \sqrt{21}$ phase. Particularly, through analyzing the STM images of precursory 2D nuclei appearing at the very initial stage of Ag adsorption, which lead to the $\sqrt{21} \times \sqrt{21}$ phase by their coalescence, and also by analyzing the STM images of their out-of-phase domain boundaries, it is most likely that the Ag adatoms sit on the Ag-trimer centers of the initial $\sqrt{3} \times \sqrt{3}$ -Ag framework. This conclusion seems to be consistent with the previous photoemission results [13]. Further, by comparing the STM images of the $\sqrt{21} \times \sqrt{21}$ superstructure induced by Au adsorption, taken by other groups [23,24], with our STM images of Ag adsorption, it is suggested that the Ag-induced and Au-induced $\sqrt{21} \times \sqrt{21}$ structures have a very similar atomic arrangement.

2. Experimental

We used two separate ultrahigh vacuum (UHV) chambers: one had a RHEED (reflection-high-energy electron diffraction) system, enabling in-situ observations during Ag deposition at substrate temperatures of 90–1500 K. This was the same one used in the previous works [1,3,6,11,12]. Another chamber had a low-temperature STM system (UNISOKU USM-501 type) down to 6 K,

equipped with a preparation chamber with another RHEED system. STM images shown here were taken in so-called constant-height operating mode only with slow feed back in tip motion. The tip-bias voltage V_t and the tunneling current I_t for each image are indicated in the figure captions. Every chambers had alumina-coated W baskets as Ag evaporators. The base pressures were about 5×10^{-11} Torr, and could be kept less than 5×10^{-10} Torr during depositions. The substrate was a p-type Si(111) wafer and its typical dimensions were $25 \times 1.5 \times 0.4$ mm³. A clear Si(111)- 7×7 RHEED pattern was produced by flashing the sample at 1500 K several times by passing DC current around 6 A through it. The $\sqrt{3} \times \sqrt{3}$ -Ag surface structure was prepared by 1 ML of Ag deposition with a constant rate of 0.66 ML/min onto the 7×7 substrate maintained at 650 K. The amount of the deposition was calibrated by assuming 1 ML of Ag for the complete conversion from the 7×7 to the $\sqrt{3} \times \sqrt{3}$ -Ag structures in RHEED [28]. After this preparation, the substrate was cooled down to 70 K at the STM sample stage. The liquid nitrogen container was evacuated to freeze the nitrogen for avoiding its boiling vibration. The additional Ag was deposited onto the substrate on the STM sample stage at this temperature with a rate of less than 0.1 ML/min. The temperature of the Si wafer below RT was estimated with a AuFe–Chromel thermocouple attached on the sample holder. The higher temperature range for cleaning and preparing the surface was measured with an optical pyrometer.

3. Results and discussions

3.1. Structural evolution during Ag adsorption

Fig. 1a shows a clear RHEED pattern of the initial $\sqrt{3} \times \sqrt{3}$ -Ag structure at about 150 K before additional deposition of Ag. Fig. 1b shows the RHEED pattern of the $\sqrt{21} \times \sqrt{21}$ -Ag structure, which was observed with additional Ag depositions between about 0.1 and 0.25 ML. Its most sharp pattern was obtained around 0.15–0.20 ML cover-

age. This superstructure was commonly observed at the temperatures ranging from 70 to 250 K [3]. The diffraction spots in this RHEED pattern come from two equivalent domains of the $\sqrt{21} \times \sqrt{21}$ structure with $\pm 10.89^\circ$ rotations with respect to the 1×1 fundamental lattice of Si(111) surface. Fig. 1d and e show the 2D lattices in the reciprocal and real spaces, respectively, corresponding to the $\sqrt{3} \times \sqrt{3}$ and $\sqrt{21} \times \sqrt{21}$ superstructures. Beyond 0.30 ML of Ag deposition, the $\sqrt{21} \times \sqrt{21}$ -Ag spots became weaker with polycrystalline Ag spots coexisting as shown in Fig. 1c. These RHEED observations [3] provide a guide in Ag coverage for STM observations mentioned below.

Fig. 2a shows an STM image taken from the $\sqrt{3} \times \sqrt{3}$ -Ag surface at 70 K with deposition of very small amount of additional Ag atoms. Some bright protrusions distribute randomly on the $\sqrt{3} \times \sqrt{3}$ -Ag substrate. Each bright protrusion corresponds to an adsorbed Ag monatom. By counting the average density of the additionally adsorbed Ag atoms at the central parts of terraces, we can estimate the coverage to be about 0.015 ML. The distances between the nearest neighboring adatoms are about 3 to 10 units of the $\sqrt{3} \times \sqrt{3}$ cell, namely 2–7 nm separations. The steps are boundaries between the upper and lower terraces of the $\sqrt{3} \times \sqrt{3}$ domains [29,30]. At these step edges, the Ag adatoms seem to distribute in a regular arrangement with a periodicity of about three unit meshes of the $\sqrt{3} \times \sqrt{3}$. The density of adsorbed Ag adatoms is higher at the steps than on the terraces. Near these steps, denuded zones are recognized where adsorbed monomers do not exist. The width of the denuded zone, around 3 nm, corresponds to the diffusion length of the deposited Ag atoms. It can then be indicated that the adsorbed atoms still migrate with some mobility on the $\sqrt{3} \times \sqrt{3}$ -Ag surface even at 70 K, so that they interact with the steps to be trapped. The regular arrangement along the steps can be considered owing to interaction among the Ag adatoms. It should be noted that STM observations at RT never showed the indication of additionally deposited Ag atoms of similar amounts on the $\sqrt{3} \times \sqrt{3}$ -Ag surface. This is because the adatoms migrate with an extremely high mobility, making a 2D adatom gas phase [4,5].

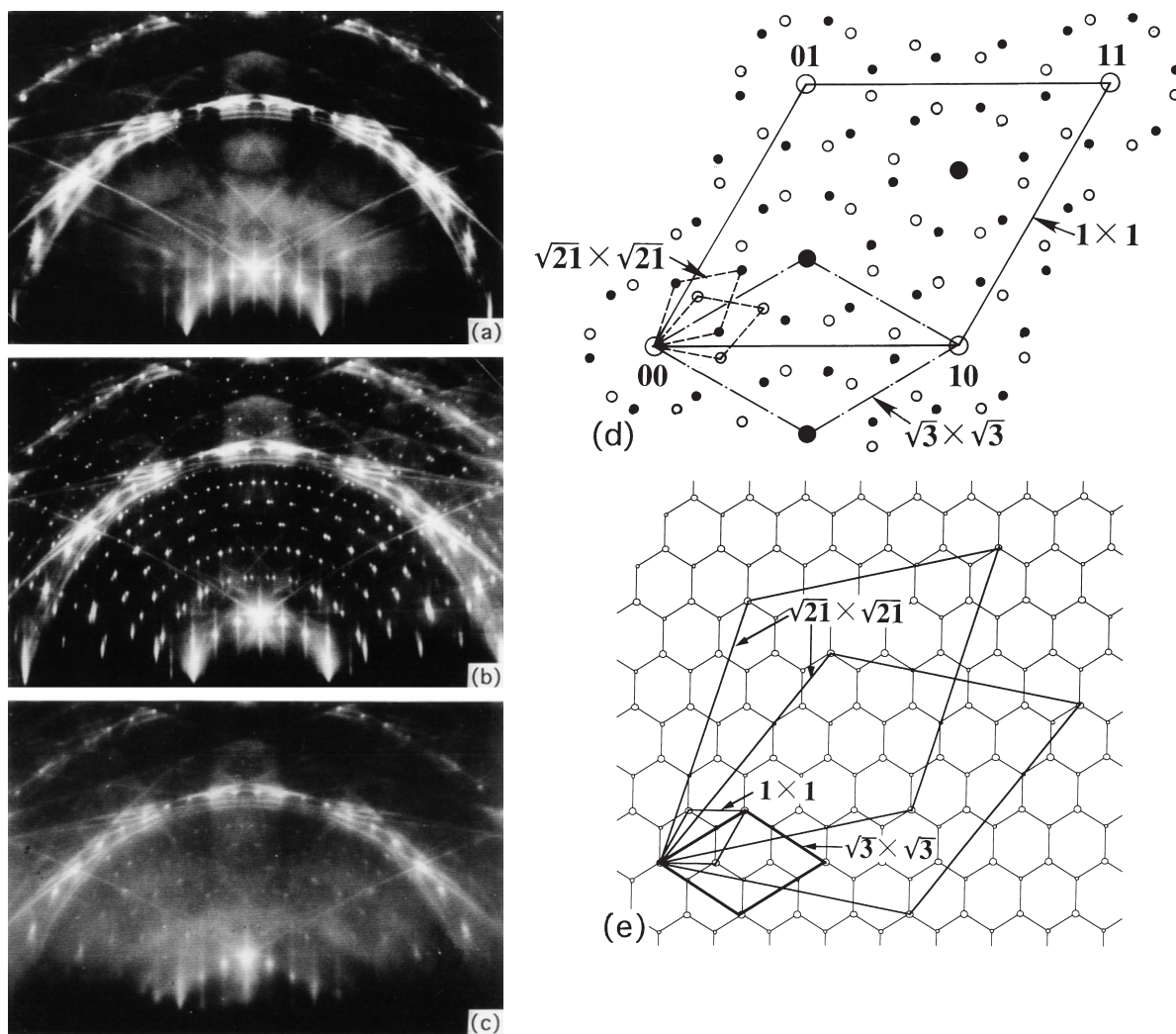


Fig. 1. RHEED patterns observed around 150 K. (a) The initial Si(111)- $\sqrt{3} \times \sqrt{3}$ -Ag surface before additional Ag adsorption. (b) Si(111)- $\sqrt{21} \times \sqrt{21}$ -Ag surface induced by approximately 0.15 ML of additional Ag adsorption on (a). (c) With further adsorption of Ag up to 0.3 ML, the $\sqrt{21} \times \sqrt{21}$ superspots are weakened. (d) Two-dimensional reciprocal- and (e) real-space lattices, respectively, for the $\sqrt{3} \times \sqrt{3}$ and $\sqrt{21} \times \sqrt{21}$ periodicities.

When we continued further deposition up to about 0.05 ML of Ag, as shown in Fig. 2b, 2D nuclei were formed at terraces and steps. This is because the monomers observed in Fig. 2a still migrate to gather into the nuclei when the adatom density exceeds some critical value. The density of 2D nuclei at steps is much higher than that on terraces. They connect with each other to form thin atomic strings along the steps.

When the Ag coverage was increased further,

the density of 2D nuclei on terraces increased, as shown in Fig. 2c. At this stage, monomers were hardly observed. With further increase of Ag coverage, the arrangements of these 2D nuclei began to be in order as shown in Fig. 2d; we recognize a disordered region A, a well-ordered regions B, and between them in order as indicated by a region C. Although the degree of ordering in these regions is different, the unit structure of 2D nuclei seems to be the same, as shown later.

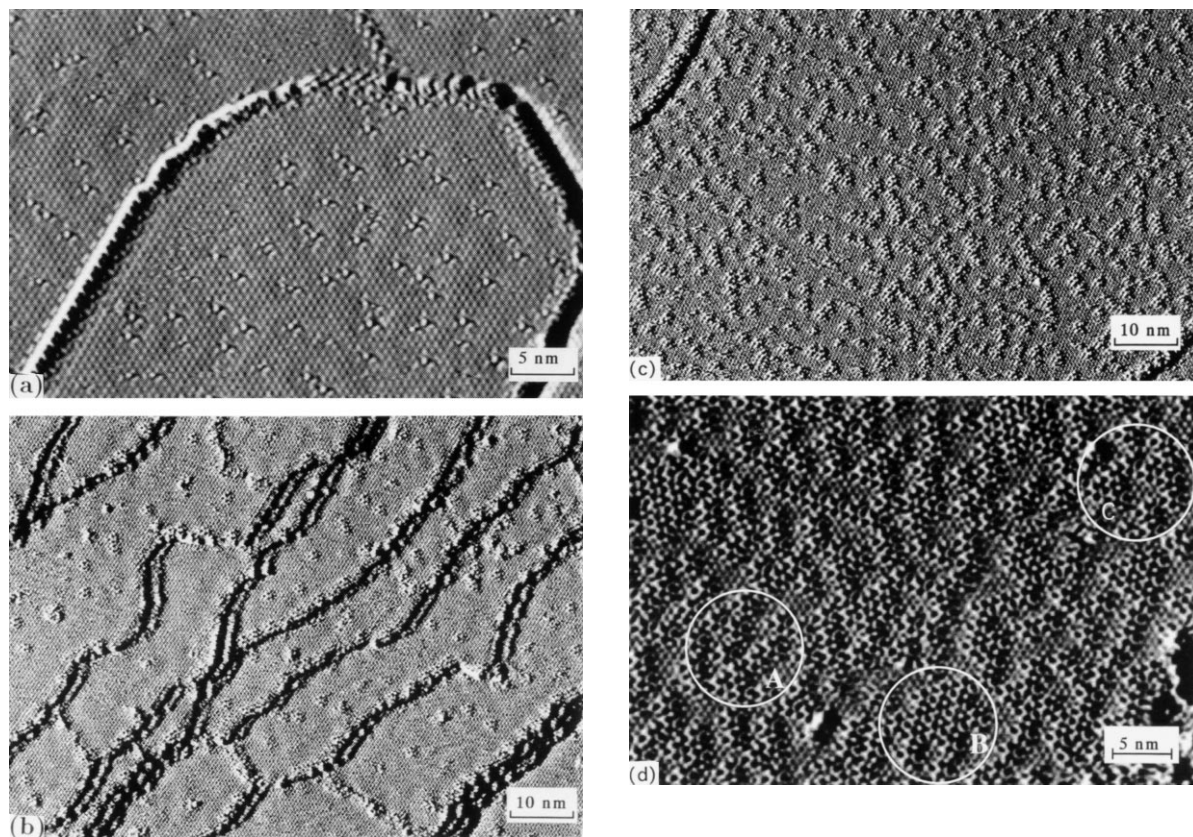
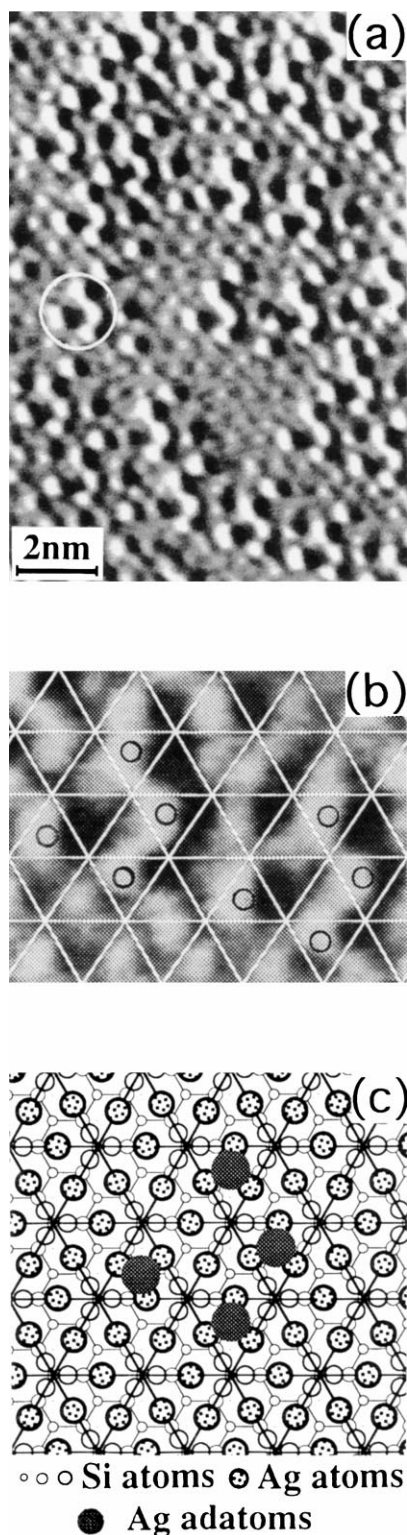


Fig. 2. Occupied-state STM images taken during Ag adsorption on the Si(111)- $\sqrt{3} \times \sqrt{3}$ -Ag surface at 70 K with tip-bias voltage $V_t = 1.0$ V and tunneling current $I_t = 0.5$ nA. The additional coverages of Ag are approximately: (a) 0.015; (b) 0.05; (c) 0.1; and (d) 0.12 ML, respectively.

Fig. 3a shows a magnified STM image taken from the $\sqrt{3} \times \sqrt{3}$ -Ag surface with approximately 0.1 ML of additional Ag atoms deposited at 70 K, which corresponds to a Ag coverage between Fig. 2c and d. The underlying substrate is the $\sqrt{3} \times \sqrt{3}$ -Ag structure, on which some 2D nuclei consisted of bright protrusions distribute randomly. In fact, characteristic protrusions indicated by a white circle are frequently seen. Fig. 3b is a magnified image of Fig. 3a, on which a grid with the $\sqrt{3} \times \sqrt{3}$ periodicity is superimposed.

The positions of the points of intersection in grid are not defined with respect to the $\sqrt{3} \times \sqrt{3}$ -Ag framework at this moment. It is seen that the protrusions are not on the points of intersection of the grid, but they are located in its triangles. Here, we recognize characteristic features

in protrusions, corresponding to two sets of 2D nuclei, each of which is consisted of four protrusions indicated by open circles in b. In order to obtain an atomic arrangement model of the 2D nuclei, we assumed that these open circles directly correspond to Ag adatoms. Then, we tried to put these Ag adatoms only on the centers of the Si trimers in the HCT (honeycomb-chained trimers) structure [14, 15] of the initial $\sqrt{3} \times \sqrt{3}$ -Ag surface. But, we could not reproduce the arrangement of the 2D nuclei of Fig. 3b by putting the adatoms only on the Si trimers. Instead, when we put the Ag adatoms only on the centers of the Ag trimers in the HCT framework, we could obtain an atomic arrangement for the 2D nuclei shown in Fig. 3c. In this model, the 2D nucleus is consisted of four Ag adatoms that are located only on the centers



of Ag trimers (Fig. 3c). The relative positions among them seem to be consistent with Fig. 3b. This is a plausible model of the 2D nuclei.

When Ag coverage arrived around 0.15 ML, the arrangement of 2D nuclei became better ordered in longer ranges, as shown in Fig. 4a, in which the $\sqrt{21} \times \sqrt{21}$ periodicity is clearly recognized as indicated by white lozenges. It can be said, thus, that the 2D nuclei mentioned above are initially formed as a precursory structure leading to the formation of the $\sqrt{21} \times \sqrt{21}$ superstructure. There are two equivalent domains with different orientations in this superstructure. They rotate $\pm 10.89^\circ$ from $[11\bar{2}]$ direction, respectively. Around 0.20 ML Ag deposition, the whole surface was covered by the $\sqrt{21} \times \sqrt{21}$ -Ag phase as shown in Fig. 4b. Each $\sqrt{21} \times \sqrt{21}$ domain is consisted of about 4×4 – 10×10 unit meshes, meaning that the domain size is about 7×7 – 20×20 nm². This is larger than the distances among the Ag monomers initially distributed in Fig. 2a and among the 2D nuclei in Fig. 2c. Many of the boundaries between the $\sqrt{21} \times \sqrt{21}$ domains are straight along the directions of $\pm 10.89^\circ$ off from $[11\bar{2}]$, i.e. along the edges of the $\sqrt{21} \times \sqrt{21}$ unit mesh. But, besides the steps, there are some domain boundaries which do not run along these directions. These may be the original domain boundaries in the initial $\sqrt{3} \times \sqrt{3}$ -Ag substrate. The details on the out-of-phase domain boundaries will be discussed in Section 3.3.

When Ag was deposited further, as shown in Fig. 5a, 3D islands were formed randomly, but in a slight preference at the domain boundaries on the $\sqrt{21} \times \sqrt{21}$ -Ag structure. Their sizes are roughly 1–2 nm. The Si(111)- $\sqrt{21} \times \sqrt{21}$ structure

Fig. 3. (a) An occupied-state STM image ($V_t=1.0$ V, $I_t=0.62$ nA) of the Si(111)- $\sqrt{3} \times \sqrt{3}$ -Ag surface at 70 K with additional Ag of approximately 0.1 ML coverage. (b) Its enlarged image showing two sets of 2D nuclei, with a superimposed grid of the $\sqrt{3} \times \sqrt{3}$ periodicity. All protrusions indicated by open circles are located in the triangles of the grid. (c) A model of the atomic arrangement for the 2D nucleus. Four additional Ag atoms (large shaded circles) adsorb on the centers of Ag trimers (medium-sized circles with dots) in the $\sqrt{3} \times \sqrt{3}$ -Ag framework. Smaller open circles indicate the Si trimers, and the smallest ones are the underlying Si bilayer of the (111) face.

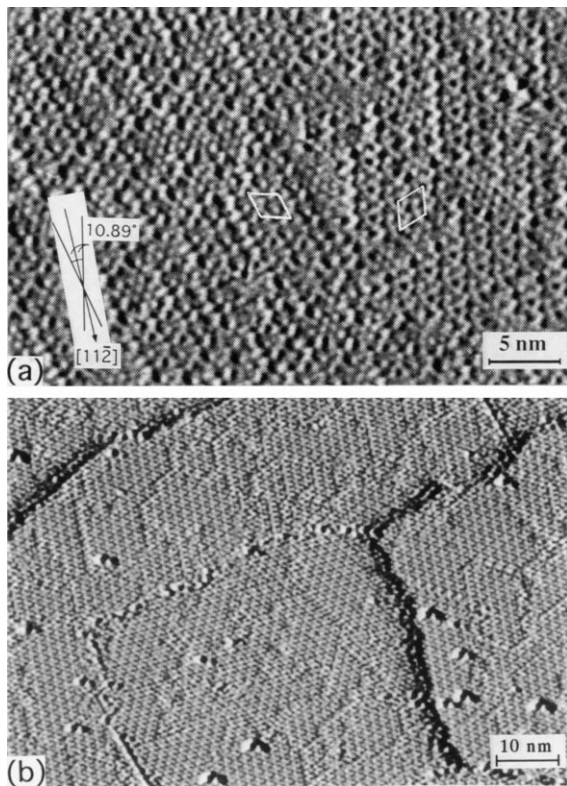


Fig. 4. (a) An empty-state STM image ($V_t = -1.0$ V, $I_t = 0.4$ nA), showing growing domains of the $\sqrt{21} \times \sqrt{21}$ -Ag structure which rotate $\pm 10.89^\circ$ from $[11\bar{2}]$ direction. The white lozenges indicate their unit cells. (b) The whole surface is covered by the $\sqrt{21} \times \sqrt{21}$ phase with additional Ag adsorption of about 0.20 ML coverage.

on the substrate surface among the islands does not seem to be destroyed as shown in a magnified image of Fig. 5b; the lozenge indicates the $\sqrt{21} \times \sqrt{21}$ unit mesh. In Fig. 5c, the whole surface is covered by the 3D islands with further deposition.

In this way, our in-situ STM observations have clearly revealed structural evolutions during Ag adsorption on the $\sqrt{3} \times \sqrt{3}$ -Ag surface at 70 K: (1) adsorption as individual monomers; (2) their nucleation into 2D nuclei; (3) their coalescence into the $\sqrt{21} \times \sqrt{21}$ superstructure; and (4) 3D islanding on it. A characteristic feature of this process is the 2D nuclei formation which is a precursory stage leading to the formation of the $\sqrt{21} \times \sqrt{21}$ structure.

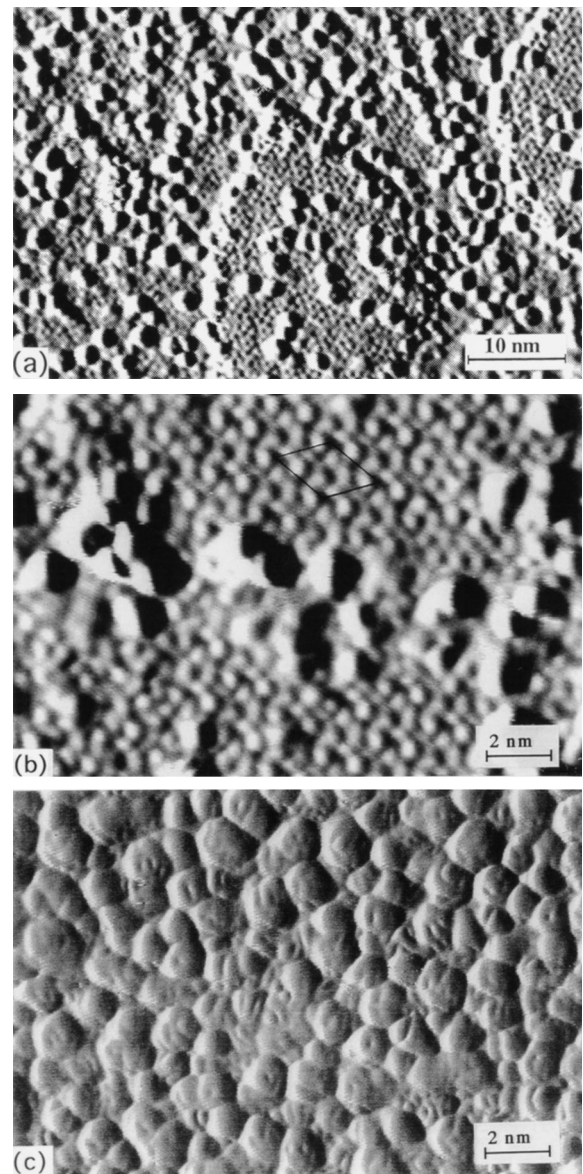
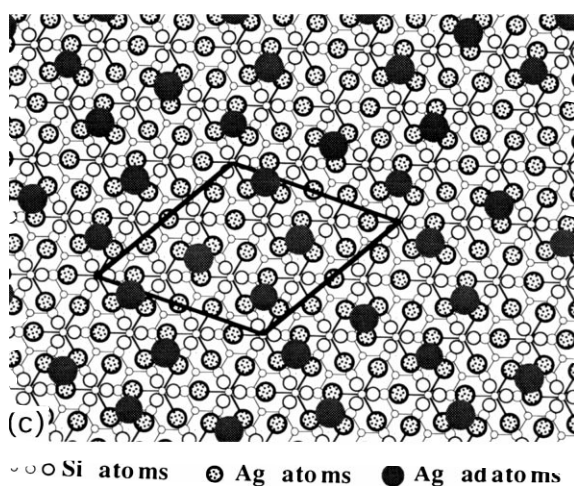
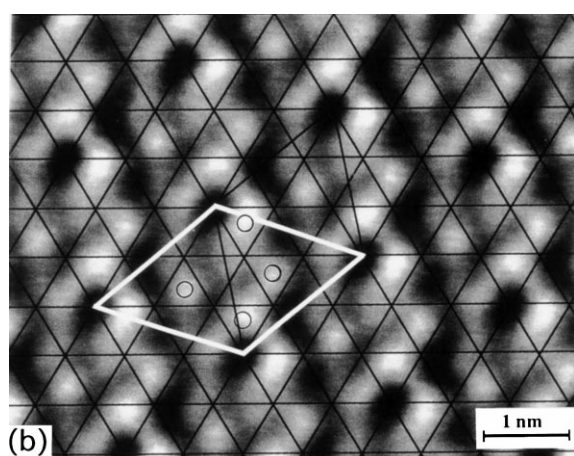
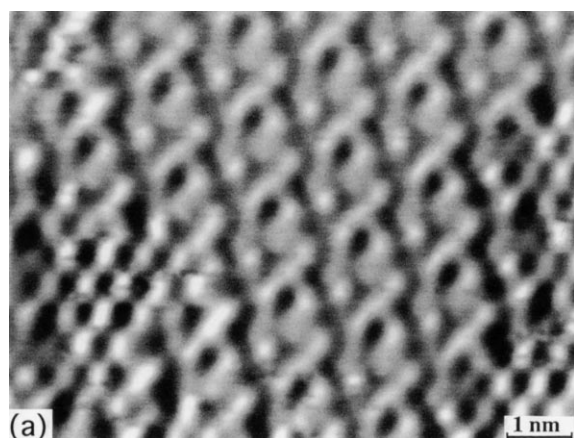


Fig. 5. (a) An occupied-state STM image ($V_t = 1.5$ V, $I_t = 0.53$ nA) of the $\sqrt{21} \times \sqrt{21}$ -Ag structure with 3D islands coexisting by further deposition beyond the saturation coverage of the superstructure. (b) Its enlarged image. (c) The surface is wholly covered by 3D islands with further Ag deposition.

3.2. Model of the $\sqrt{21} \times \sqrt{21}$ -Ag superstructure

Fig. 6a shows a magnified STM image taken from the $\sqrt{3} \times \sqrt{3}$ -Ag surface at 70 K with addi-



tional Ag deposition of around 0.15 ML. The $\sqrt{21} \times \sqrt{21}$ domains are formed with the $\sqrt{3} \times \sqrt{3}$ -Ag domains partially remained at the lower left and right corners in the image. In Fig. 6b, a triangular grid of black lines of the $\sqrt{3} \times \sqrt{3}$ periodicity is superimposed on the image of the $\sqrt{21} \times \sqrt{21}$ domain. Their points of intersection are set on the Si-trimer centers in the HCT framework of the initial $\sqrt{3} \times \sqrt{3}$ -Ag structure, as in Fig. 3c. This position of grid was determined with reference to the partially remained $\sqrt{3} \times \sqrt{3}$ -Ag domains. So, the centers of the triangles in the grid correspond to the Ag-trimer centers of the $\sqrt{3} \times \sqrt{3}$ -Ag framework. The white lines indicate the unit cell of the $\sqrt{21} \times \sqrt{21}$ structure. In the unit cell, some bright protrusions are recognized as indicated by open circles, which are roughly located in the triangles of the grid, not on the points of intersection. But, it is difficult at a glance to judge whether these bright protrusions come from the newly adsorbed Ag adatoms or come from the Ag trimers of the initial $\sqrt{3} \times \sqrt{3}$ -Ag substrate. (It is known that the Ag-trimer centers of the $\sqrt{3} \times \sqrt{3}$ -Ag structure produce bright protrusions in empty-state STM images owing to the maxima in local density of states [31,20–22]. These protrusions, if remained, should be located at the centers of the triangles in the grid in this figure.) Although, however, the relative intensities among the bright protrusions changed depending on the tip-bias voltage, their positions indicated by open circles in Fig. 6b remained unchanged for both the empty- and filled-states images. Nogami et al. [23] also report that the features in STM images are the same in both of empty- and filled-states images. On the other hand, in the HCT model of the $\sqrt{3} \times \sqrt{3}$ -Ag structure, the protrusions in the empty-state STM images correspond to the centers of Ag trimers as mentioned above, while the protrusions in the filled-state STM images corre-

Fig. 6. (a) An empty-state STM image ($V_t = -1.6$ V, $I_t = 0.5$ nA) of the $\sqrt{3} \times \sqrt{3}$ -Ag surface with additional Ag adsorption of approximately 0.15 ML. The domain of $\sqrt{21} \times \sqrt{21}$ superstructure is clearly recognized. (b) Its enlarged image of the $\sqrt{21} \times \sqrt{21}$ domain with a superimposed grid of the $\sqrt{3} \times \sqrt{3}$ periodicity. (c) A proposed model for the atomic arrangement in the $\sqrt{21} \times \sqrt{21}$ superstructure.

spond to the positions of the Ag atoms themselves [31]. So, we can conclude that bright protrusions in the $\sqrt{21} \times \sqrt{21}$ domains in Fig. 6b do not correspond to the Ag-trimer centers of the remained $\sqrt{3} \times \sqrt{3}$ -Ag framework, rather they are considered to directly correspond to the positions of the additional Ag adatoms.

By comparing the distribution of bright protrusions in the unit cells in Fig. 6b with the structure of a 2D nucleus in Fig. 3b, we can find that they are the same arrangement with each other. That is to say, the $\sqrt{21} \times \sqrt{21}$ -Ag domains are constructed through a regular arrangement of the 2D nuclei that appear at the very initial stage of adsorption.

According to the above experimental results and analysis, we can obtain a structural model of the $\sqrt{21} \times \sqrt{21}$ superstructure, as shown in Fig. 6c. In this simplest possible model, it is assumed that additional Ag atoms sit on the Ag-trimer centers in the unaltered $\sqrt{3} \times \sqrt{3}$ -Ag framework, which seems plausible by considering the previous studies mentioned in the Introduction. The topmost layer is consisted of these Ag adatoms. An $\sqrt{21} \times \sqrt{21}$ unit mesh has four newly adsorbed Ag adatoms. The saturation coverage for additional Ag is then $4/21 = 0.19$ ML which is roughly consistent with the observation of RHEED in Fig. 1.

Then, a simple question will be raised; why do the Ag adatoms sit on the Ag trimers, not on the Si trimers or at the other sites? This question can be answered by understanding how the adatoms are bonded with the $\sqrt{3} \times \sqrt{3}$ -Ag substrate. With the aid of the photoemission data for the Au-induced $\sqrt{21} \times \sqrt{21}$ superstructure [13] and by considering the similarity in structure between the Au- and Ag-induced $\sqrt{21} \times \sqrt{21}$ phases, we can guess the answer as follows. Although there are no dangling bonds on the $\sqrt{3} \times \sqrt{3}$ -Ag surface, there is an anti-bonding surface-state band, called S_1 band, of which local density of states has maxima at the Ag-trimer centers of the HCT framework [18–22,31]. This surface-state band is partly (about 3%) filled with electrons [13,18,19], so that we can detect it by photoemission spectroscopy. Recently, we found that when a small amount of Ag or Au (less than 0.1 ML) was

deposited onto the $\sqrt{3} \times \sqrt{3}$ -Ag surface, the photoemission intensity from the S_1 band was strengthened, and the bottom of the S_1 band shifted downwards below the Fermi level [13,32,5]. This means that the adsorbed Ag or Au atoms dope electrons into the S_1 band so that the filling of the band increases. When Au was further deposited, with the appearance of the $\sqrt{21} \times \sqrt{21}$ structure, the S_1 band splits into two bands, called S_1^* and S_1' bands [13]. According to the band bending in the surface space-charge layer measured by bulk-sensitive XPS (X-ray photoelectron spectroscopy) [13,32], it can be said that the electrons trapped in the S_1^* and S_1' bands of the $\sqrt{21} \times \sqrt{21}$ structure are donated from the Au adatoms, not come from the bulk. This means that the adatoms are positively ionized. Then, owing to the Coulomb attraction between the ionized adatoms and the negative charge background at the S_1^* and S_1' bands of the substrate, a stable surface bonding are formed [13,32]. This is the reason why Au adatoms sit on the Ag trimers, not on the Si trimers. The Si trimers do not possess an anti-bonding state like the Ag trimers have. As mentioned below, the $\sqrt{21} \times \sqrt{21}$ superstructures induced by Au adsorption at RT [2,23–25] and by Ag adsorption at lower temperatures [1,3] seem to have the same atomic arrangement. Therefore, the evolutions of the surface electronic structures are considered to be similar to each other, so that the reason why the Ag adatoms sit on the Ag trimers may be the same as in the case of Au-induced $\sqrt{21} \times \sqrt{21}$ structure.

For the $\sqrt{21} \times \sqrt{21}$ structure induced by Au deposition onto the $\sqrt{3} \times \sqrt{3}$ -Ag surface at RT, Nogami et al. [23]. and Ichimiya et al. [24] suggested different atomic arrangement models. Our proposed model in Fig. 6c for the $\sqrt{21} \times \sqrt{21}$ structure induced by Ag adsorption, instead of Au, is different from that of Nogami and Ichimiya. In Nogami's model, as shown in Fig. 7b, the $\sqrt{21} \times \sqrt{21}$ unit cell contains five adatoms sitting on the Ag trimers, while in Ichimiya's model (Fig. 7c) the unit cell contains three adatoms sitting on the Si trimers. These models are different from ours, shown in Fig. 7a, where the unit cell contains four adatoms sitting on the Ag trimers.

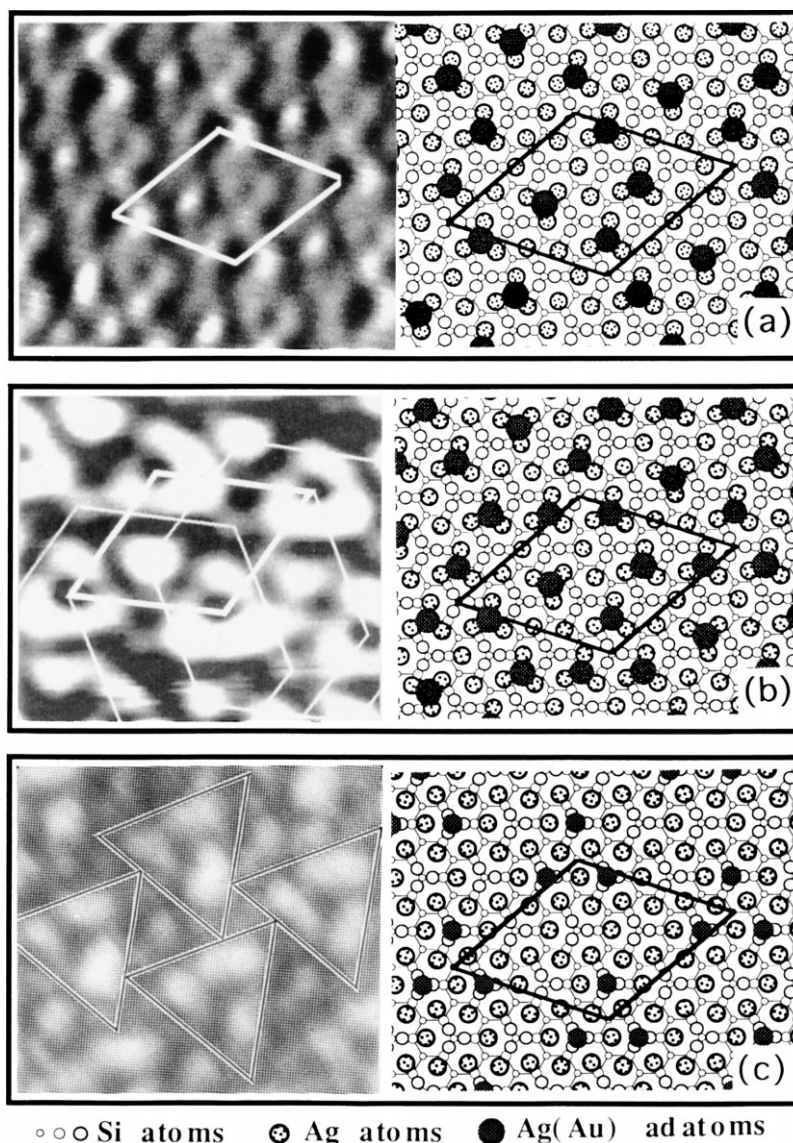


Fig. 7. Comparison of STM images between Ag-induced and Au-induced $\sqrt{21} \times \sqrt{21}$ superstructures. Right panels show the proposed model by the respective authors. (a) Our STM image and model for the Ag-induced $\sqrt{21} \times \sqrt{21}$ phase. (b) Those of Nogami et al. [23] for the Au-induced $\sqrt{21} \times \sqrt{21}$ phase. (c) Those of Ichimiya et al. [24] for the Au-induced $\sqrt{21} \times \sqrt{21}$ phase.

However, by comparing the STM images of ours and those of the $\sqrt{21} \times \sqrt{21}$ -(Ag+Au) surface obtained by Nogami et al. and Ichimiya et al., they look very similar to each other as shown on the left panels in Fig. 7; there are triangular-like protrusions around corner holes of the unit cell, and a prominent protrusion only in the center of

the half unit-cell triangle. Nogami et al. assumed that five protrusions observed in the $\sqrt{21} \times \sqrt{21}$ unit cell (though one of them is much weaker than the other four) directly correspond to the adatoms, based on their dual-polarity STM images and the saturation coverage of 0.24 ML they measured. On the other hand, Ichimiya et al. assumed three

adatoms in the unit cells because of its saturation coverage of 0.15 ML they measured. Four protrusions in the unit cell in the images were attributed to some effects of electronic structures, not directly to the adatoms, by considering the results of rocking-curve measurements in RHEED. Our model is, however, derived by assuming the saturation coverage of about 0.2 ML and four protrusions in the images to be adatoms. These assumptions are supported by analyzing the 2D nuclei at a precursory stage for the $\sqrt{21} \times \sqrt{21}$ structure mentioned above, and the structure of the out-of-phase domain boundaries mentioned in the next subsection.

The former two models are for the Au-induced $\sqrt{21} \times \sqrt{21}$ superstructure at RT, while ours is for the Ag-induced one at low temperatures. So, one may expect some difference in structure between them. But, Ichimiya et al. measured the RHEED rocking curves from both of the Au- and Ag-induced $\sqrt{21} \times \sqrt{21}$ structures [33]. Since the both curves had similar profiles, it was concluded that Ag adatoms occupied the same sites as the Au adatoms did. This supports our conclusion that the atomic arrangement structures of the Ag-induced and Au-induced $\sqrt{21} \times \sqrt{21}$ superstructures are the same.

3.3. Out-of-phase domain boundaries

Fig. 8a shows out-of-phase domain boundaries between three $\sqrt{21} \times \sqrt{21}$ -Ag domains. They are running in two different orientations, 10.89° off from $[10\bar{1}]$ and $[11\bar{2}]$ directions, as indicated by arrows. The structures on both sides of the boundary are equivalent. The shift between the domains is about 7 \AA , which corresponds to $\sqrt{3}a = 6.65 \text{ \AA}$ shift along $[10\bar{1}]$ or $[11\bar{2}]$ direction. At the boundaries, the $\sqrt{3} \times \sqrt{3}$ -Ag structure is partly observed. This means that it is slightly less than the saturation coverage of the $\sqrt{21} \times \sqrt{21}$ superstructure. Fig. 8b shows another example almost exactly at the saturation coverage where the $\sqrt{21} \times \sqrt{21}$ periodicity comes up right at the boundaries.

Fig. 9b shows a model of the atomic arrangement near the domain boundaries corresponding to the STM image of Fig. 9a. It indicates that all

of Ag adatoms are located on the Ag trimers of the underlying $\sqrt{3} \times \sqrt{3}$ -Ag framework. Such an arrangement cannot be reproduced by putting the Ag adatoms only on top of the Si-trimer centers. This is another reason why we believe that Ag adatoms sit on the Ag-trimer centers. The two staggered domains have the same structures, but are only different in the phase of periodicity relative to the substrate.

Many of the out-of-phase domain boundaries of the $\sqrt{21} \times \sqrt{21}$ superstructure, as seen in Fig. 4b, are not considered to be associated with the domain boundaries on the initial $\sqrt{3} \times \sqrt{3}$ -Ag surface [30,34] for the following reasons. First, the domain size of the initial $\sqrt{3} \times \sqrt{3}$ surface is much larger than the size of the $\sqrt{21} \times \sqrt{21}$ domains. Second, the domain boundaries on the $\sqrt{3} \times \sqrt{3}$ surface generally align along the $[11\bar{2}]$ directions, i.e. along the edge of the $\sqrt{3} \times \sqrt{3}$ unit cell, while the boundaries of the $\sqrt{21} \times \sqrt{21}$ domains are along the $[11\bar{2}]$ $R \pm 10.89^\circ$, i.e. along the edge of the $\sqrt{21} \times \sqrt{21}$ unit mesh. So, we can conclude that the initial $\sqrt{21} \times \sqrt{21}$ domains are formed through coalescence of the 2D nuclei shown in Fig. 3. The domain growth proceeds by coalescing the neighboring tiny $\sqrt{21} \times \sqrt{21}$ domains with the same phase relative to the substrate. But, when the domains with different phases face each other, the out-of-phase domain boundaries are formed between them. They tend to be straight owing to a positive formation energy of the boundary.

4. Summary

(1) We have revealed the following structural evolutions through in-situ STM observations during Ag adsorption onto the Si(111)- $\sqrt{3} \times \sqrt{3}$ -Ag surface at 70 K. In the range of additional Ag coverage less than 0.02 ML, the Ag adatoms distributed randomly as monomers on the $\sqrt{3} \times \sqrt{3}$ -Ag surface. This is because the surface migration of Ag adatoms is sufficiently suppressed that they look fixed in a time-scale for STM imaging. Its density was higher at steps than on terraces. With increase of Ag coverage up to around

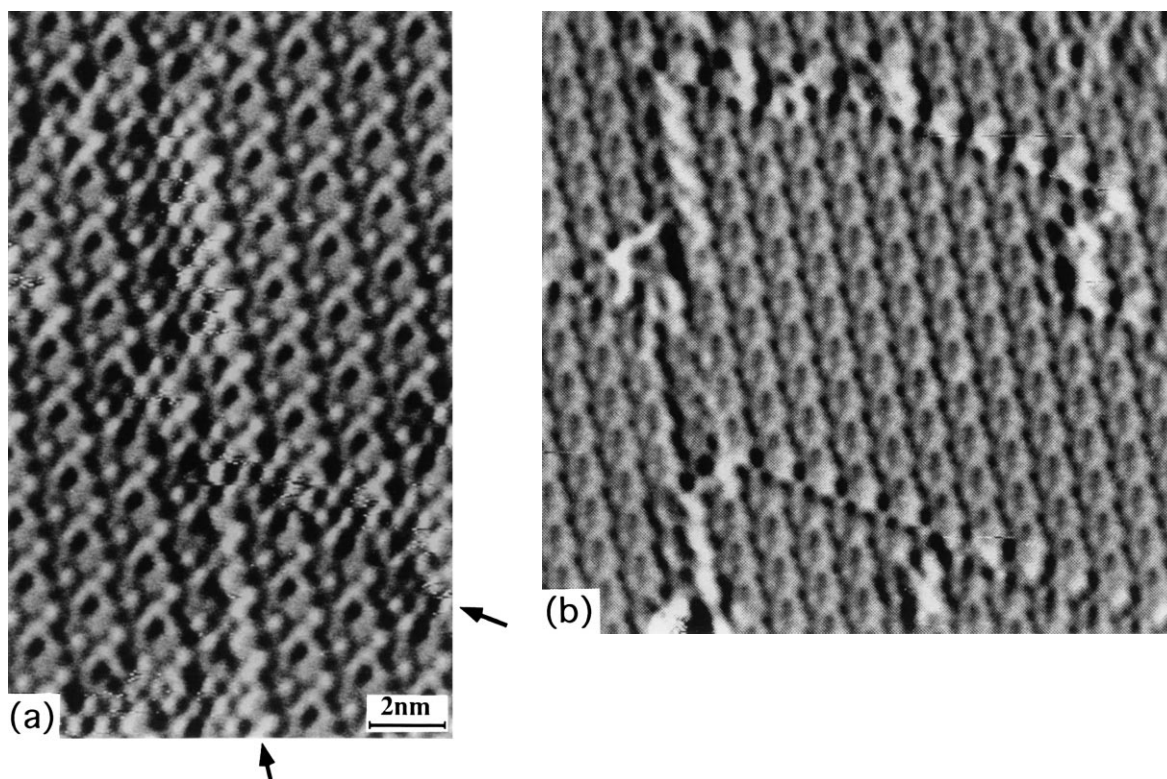


Fig. 8. (a) An empty-state image of the $\sqrt{21} \times \sqrt{21}$ -Ag surface with out-of-phase domain boundaries ($V_t = -1.2$ V, $I_t = 0.6$ nA). (b) That with slight increase in Ag coverage ($V_t = -1.0$ V, $I_t = 0.66$ nA).

0.1 ML, the 2D nuclei consisting of four Ag adatoms appeared, the density of which was much higher at steps than on terraces. This means that the surface migration of the Ag adatoms observed as monomers in the very initial stage do not completely freeze, but they still migrate to nucleate even at 70 K. In the coverage range from 0.1 to 0.2 ML, a $\sqrt{21} \times \sqrt{21}$ -Ag superstructure with orientations in $\pm 10.89^\circ$ from $[11\bar{2}]$ directions appeared. Their domain sizes were about 7×7 – 16×16 nm². This superstructure was formed through periodic arrangements of the 2D nuclei. The 3D Ag islands began to nucleate on the unaltered $\sqrt{21} \times \sqrt{21}$ surface with excess Ag depositions beyond the saturation coverage of the superstructure.

(2) We have proposed a structural model for the $\sqrt{21} \times \sqrt{21}$ -Ag superstructure by considering the 2D nuclei appearing at the initial stage of adsorption, and also by considering a structure of

their out-of-phase domain boundaries. Its unit mesh is consisted of four newly adsorbed Ag adatoms located on the center of Ag trimers of the $\sqrt{3} \times \sqrt{3}$ -Ag substrate. The $\sqrt{3} \times \sqrt{3}$ -Ag framework is conserved underlying in the $\sqrt{21} \times \sqrt{21}$ phase.

(3) We have observed the out-of-phase domain boundaries of the $\sqrt{21} \times \sqrt{21}$ phase. Their atomic arrangements are consistently understood by using our structural model of the $\sqrt{21} \times \sqrt{21}$ superstructure. That is to say, they seem to be consistent to the model that Ag adatoms sit on the Ag-trimer centers.

(4) By comparing the STM images of the $\sqrt{21} \times \sqrt{21}$ phase induced by Au adsorption, taken by other groups, and ours for Ag adsorption, it is suggested that both of the $\sqrt{21} \times \sqrt{21}$ phases have a very similar atomic arrangement. This similarity is also supported by the measurements of RHEED rocking curves by Ichimiya et al. [33].

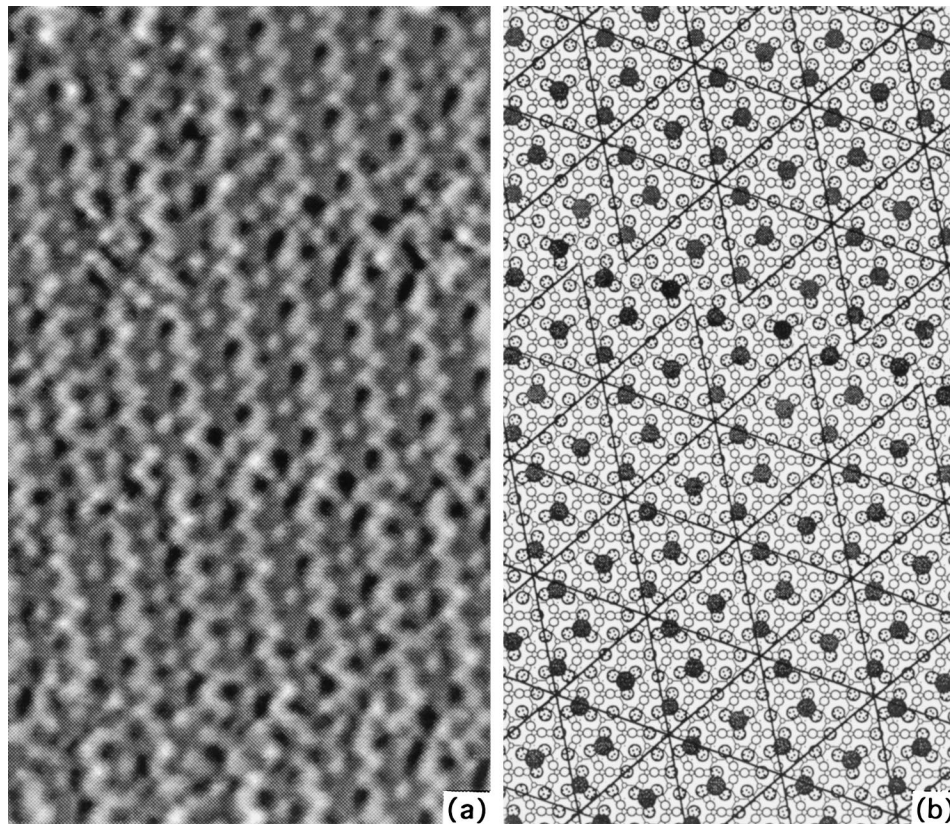


Fig. 9. (a) An empty-state STM image ($V_t = -1.2$ V, $I_t = 0.4$ nA) of the $\sqrt{2} \times \sqrt{2}$ -Ag phase with out-of-phase domain boundaries. (b) Its atomic arrangement model.

Acknowledgements

We acknowledge valuable discussion with Professor Martin Henzler of Hannover University. This work has been supported in part by Grants-In-Aid from the Ministry of Education, Science, Culture, and Sports of Japan, especially through the New Frontier Program Grants-In-Aid for Scientific Research (nos. 08NP1201 and 09NP1201) and the International Scientific Research Program (no. 07044133) conducted by Professor Katsumichi Yagi of Tokyo Institute of Technology. We have also been supported by CREST (Core Research for Evolutional Science and Technology) of the Japan Science and Technology Corporation (JST) conducted by Professor Masakazu Aono of Osaka University and RIKEN.

References

- [1] Z.H. Zhang, S. Hasegawa, S. Ino, Phys. Rev. B 52 (1995) 10760.
- [2] C.-S. Jiang, X. Tong, S. Hasegawa, S. Ino, Surf. Sci. 376 (1997) 69.
- [3] X. Tong, S. Hasegawa, S. Ino, Phys. Rev. B 55 (1997) 1310.
- [4] Y. Nakajima, G. Uchida, T. Nagao, S. Hasegawa, Phys. Rev. B 54 (1996) 14134.
- [5] Y. Nakajima, X. Tong, T. Nagao, S. Takeda, S. Hasegawa, Phys. Rev. B 56 (1997) 6782.
- [6] S. Hasegawa, X. Tong, C.-S. Jiang, Y. Nakajima, T. Nagao, Surf. Sci. 386 (1997) 322.
- [7] S. Hasegawa, S. Ino, Phys. Rev. Lett. 68 (1992) 1192.
- [8] S. Hasegawa, S. Ino, Surf. Sci. 283 (1993) 438.
- [9] S. Hasegawa, S. Ino, Thin Solid Films 228 (1993) 113.
- [10] S. Hasegawa, S. Ino, Int. J. Mod. Phys. B 7 (1993) 3817.
- [11] S. Hasegawa, Z.H. Zhang, C.S. Jiang, S. Ino, in: H. Sakaki, H. Noge (Eds.), Nanostructures and Quantum Effects, Springer, Berlin, 1994, p. 104.
- [12] S. Hasegawa, C.-S. Jiang, X. Tong, Y. Nakajima, Adv. Colloid Interface Sci. 71/72 (1997) 125.

- [13] X. Tong, C.-S. Jiang, S. Hasegawa, Phys. Rev. B 57 (1998) 9015.
- [14] T. Takahashi, S. Nakatani, Surf. Sci. 283 (1993) 17, and references therein.
- [15] M. Katayama, R.S. Williams, M. Kato, E. Nomura, M. Aono, Phys. Rev. Lett. 66 (1991) 2762.
- [16] T. Yokotsuka, S. Kono, S. Suzuki, T. Sagawa, Surf. Sci. 127 (1983) 35.
- [17] J.M. Nicholls, F. Salvan, B. Reihl, Phys. Rev. B 34 (1986) 2945.
- [18] L.S.O. Johansson, E. Landemark, C.J. Karlsson, R.I.G. Uhrberg, Phys. Rev. Lett. 63 (1989) 2092.
- [19] L.S.O. Johansson, E. Landemark, C.J. Karlsson, R.I.G. Uhrberg, Phys. Rev. Lett. 69 (1992) 2451.
- [20] Y.G. Ding, C.T. Chan, K.M. Ho, Phys. Rev. Lett. 67 (1991) 1454.
- [21] Y.G. Ding, C.T. Chan, K.M. Ho, Phys. Rev. Lett. 69 (1992) 2452.
- [22] S. Watanabe, M. Aono, M. Tsukada, Phys. Rev. B 44 (1991) 8330.
- [23] J. Nogami, K.J. Wan, X.F. Lin, Surf. Sci. 306 (1994) 81.
- [24] A. Ichimiya, H. Nomura, Y. Horio, T. Sato, T. Sueyoshi, M. Iwatsuki, Surf. Rev. Lett. 1 (1994) 1.
- [25] T. Nakayama, D.-H. Huang, M. Aono, Microelectr. Engng 32 (1996) 91.
- [26] I. Homma, Y. Tanishiro, K. Yagi, in: S.Y. Tong, M.A. Van Hove, K. Takayangi, X.D. Xie (Eds.), The Structure of Surfaces III, Springer, Berlin, 1991, p. 610.
- [27] K. Toriyama, T. Nagao, S. Hasegawa, to be published.
- [28] S. Hasegawa, H. Daimon, S. Ino, Surf. Sci. 186 (1987) 138.
- [29] A. Shibata, K. Takayanagi, Jap. J. Appl. Phys. 32 (1993) 1385.
- [30] D.W. McComb, R.A. Wolkow, P.A. Hackett, Phys. Rev. B 50 (1994) 269.
- [31] K.J. Wan, X.F. Lin, J. Nogami, Phys. Rev. B 45 (1992) 9509.
- [32] X. Tong, Thesis, University of Tokyo, 1997.
- [33] M. Lijadi, H. Iwashige, A. Ichimiya, Surf. Sci. 357/358 (1996) 51.
- [34] T. Nakayama, S. Watanabe, M. Aono, Surf. Sci. 344 (1995) 143.